



**HAL**  
open science

# A Comprehensive Analysis of AlN spacer and AlGaN n-doping effects on the 2DEG Resistance in AlGaN/AlN/GaN Heterostructures

C. Piotrowicz, B. Mohamad, B. Rrustemi, N. Malbert, M. A. Jaud, W. Vandendaele, M. Charles, R. Gwoziecki

## ► To cite this version:

C. Piotrowicz, B. Mohamad, B. Rrustemi, N. Malbert, M. A. Jaud, et al.. A Comprehensive Analysis of AlN spacer and AlGaN n-doping effects on the 2DEG Resistance in AlGaN/AlN/GaN Heterostructures. *Solid-State Electronics*, 2022, 194, pp.108322. 10.1016/j.sse.2022.108322 . hal-03722735

**HAL Id: hal-03722735**

**<https://hal.science/hal-03722735>**

Submitted on 5 Aug 2022

**HAL** is a multi-disciplinary open access archive for the deposit and dissemination of scientific research documents, whether they are published or not. The documents may come from teaching and research institutions in France or abroad, or from public or private research centers.

L'archive ouverte pluridisciplinaire **HAL**, est destinée au dépôt et à la diffusion de documents scientifiques de niveau recherche, publiés ou non, émanant des établissements d'enseignement et de recherche français ou étrangers, des laboratoires publics ou privés.

# A Comprehensive Analysis of AlN spacer and AlGaN n-doping effects on the 2DEG Resistance in AlGaN/AlN/GaN Heterostructures

C.Piotrowicz\*+, B.Mohamad\*, B.Rrustemi\*, N.Malbert+, M.-A.Jaud\*, W.Vandendaele\*, M.Charles\*, R.Gwoziecki\*

\*CEA, LETI, MINATEC Campus, F-38054 and Univ. Grenoble Alpes, F-38000 Grenoble, France

+University of Bordeaux, IMS Laboratory, CNRS UMR 5218, F-33400 Talence, France;

[clementine.piotrowicz@cea.fr](mailto:clementine.piotrowicz@cea.fr)

## 1. Abstract

In this paper, several epitaxial variations influencing the bi-dimensional electron gas (2DEG) are investigated. The effects of n-doped AlGaN barrier and AlN spacer thickness are studied by examining the sheet electron density ( $n_s$ ) and the mobility ( $\mu_s$ ) of the 2DEG using  $I_D(V_G)$  and  $C(V_G)$  measurements, and 1D Schrödinger-Poisson (1DSP) simulations. Specifically, the correlations between the resistance,  $\mu_s$ ,  $n_s$  and the polarization interface charges ( $\sigma$ ) are studied. Besides the well-reported benefits of the AlN spacer on  $n_s$ , we show that a thicker AlN spacer leads to larger  $n_s$  due to the enhancement of the AlN polarization. In addition, we prove experimentally that an n-doped AlGaN barrier does not significantly improve the 2DEG density but leads to the formation of a second channel in the AlGaN barrier for negative gate voltage ( $V_G \leq 0V$ ), driving the overall improvement of the resistance.

*Keywords:* AlGaN/AlN/GaN heterostructure; 2DEG; AlN spacer; n-doped AlGaN; Schrödinger-Poisson simulations; Measurements.

## 2. Introduction

GaN HEMT technology based on AlGaN/AlN/GaN heterostructures on 200 mm diameter Si (111) substrate has aroused a lot of interest for power electronics. Thanks to their crystal and polarization properties, III-N materials are very promising due to high breakdown field and excellent transport properties. To further increase the output power in HEMTs, the resistance of the bi-dimensional electron gas channel ( $R_{2DEG}$ ) needs to be reduced as far as possible. This improvement can be achieved through either  $n_s$  or  $\mu_s$  enhancement. The AlN spacer between the AlGaN and GaN layer is known to increase the  $n_s$ , but its physical root cause is not clearly identified [1,2]. In addition, the effect of n-doped AlGaN on the  $n_s$  is investigated [3-6].

## 3. Experiments

In this work, four different epitaxial-variations grown by MOCVD are investigated. **Figure 1(a)** depicts a cross-section of the studied structure, where the AlN spacer thickness ( $t_{AlN}$ ) and the n-type AlGaN doping ( $N_D$ ) are the key parameters of this study. Samples variations are summarized in **Figure 1(b)** and **Figure 1(c)** is a top view of the tested normally-ON Van der Pauw structure.

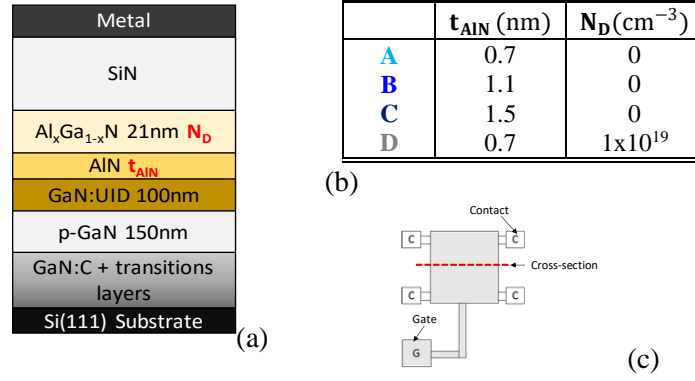


**Figure 1:** (a) Cross-section of the studied structure (b) Summary table of epitaxial variations (c) Top view of gated Van der Pauw test structure (200 $\mu$ m x 200 $\mu$ m).

In this work,  $I_D(V_G)$  and  $C(V_G)$  measurements are performed and reported for all the splits (A,B,C,D) in **Figure 2**. The  $V_{th1}$  in this article is defined as the gate voltage at which the 2DEG channel is depleted and  $V_{th2}$  is the gate voltage required to form a channel inside the AlGa<sub>N</sub> barrier.  $I_D(V_G)$  characteristics show firstly a  $V_{th1}$  variation toward negative values when  $t_{AlN}$  is increased. Moreover, an n-doped AlGa<sub>N</sub> barrier leads to an even more negative  $V_{th1}$  value and to a higher current density at  $V_G=0V$  compared to the undoped cases. Comparison with  $C(V_G)$  measurements confirms these electrostatic effects observed on  $I_D(V_G)$  curves. **Table 1(a)** reports the extractions of  $R_{2DEG}$ ,  $n_s$  and  $\mu_s$ , performed from the  $I_D(V_G)$  and  $C(V_G)$  according to equations 1 to 4. For samples A, B and C, extractions at  $V_G=0V$  refer directly to 2DEG parameters, where  $n_s$  is calculated by Eq.1 from the  $C(V_G)$  and  $R_{2DEG}$  with Eq.2 from the  $I_D(V_G)$ . Finally,  $\mu_s$  is calculated with Eq.3. As reported in **Table 1(a)**,  $n_s$  increases with larger AlN spacer but  $R_{2DEG}$  enhancement is limited by mobility degradation, likely due to the rise of surface roughness.

$$n_s (2DEG) = \frac{1}{q} \int_{V_{th1}}^V C. dV \Big|_{V=\begin{cases} 0 & \text{if } V_{th2} \geq 0V \\ V_{th2} & \text{if } V_{th2} \ll 0V \end{cases}} \quad (1)$$

$$R_{2DEG,tot} = \frac{\pi}{\ln(2)} \cdot \frac{\Delta V}{I} \quad (2)$$

$$\mu_{s,tot} = \frac{1}{q \cdot R_{2DEG,tot} \cdot n_{s,tot}} \quad (3)$$

Regarding the n-doped AlGa<sub>N</sub> sample, the extraction of the 2DEG parameters are indirect because n-doping leads to an earlier formation of the second channel in AlGa<sub>N</sub> (for  $V_G \ll 0V$ , see **Figure 4(d)**). Consequently, the extraction at  $V_G=0V$  accounts for the 2DEG and the AlGa<sub>N</sub> channel as details in **Table 1(b)**.  $n_s(\text{total})$  refers to the value extracted at  $V_G=0V$  corresponding to the sum of both channels (Eq.4).  $R_{2DEG}$  is extracted at  $V_{th2}$  before the formation of the n-AlGa<sub>N</sub> channel and  $R_{AlGaN}$  is deduced using Eq.5, where  $R_{tot}$  is the resistance at  $V_G=0V$ .

$$n_s (\text{total}) = \frac{1}{q} \int_{V_{th1}}^0 C. dV \quad (4)$$

$$R_{AlGaN} = \frac{R_{tot} \cdot R_{2DEG}}{R_{2DEG} - R_{tot}} \quad (5)$$

Surprisingly, the  $n_s(2DEG)$  barely increases with doping and the  $R_{2DEG}$  reduction is caused by a mobility degradation, likely induced by the high level of doping near the 2DEG channel. Depicted in Figure 4, the simulations of the electron density as a function of the depth for the four-studied samples explain and validate this weak rise of  $n_s$  for the doped AlGa<sub>N</sub>. Indeed, since the onset of charge density in the AlGa<sub>N</sub> barrier occurs near the AlGa<sub>N</sub>/AlN interface and thus near the 2DEG channel, a variation of the gate voltage will induce a simultaneous variation of both channels. We attribute the difference between the doped and undoped sample

to the enhance electric field in the AlGaN near the interface induced by the high level of donors. Hence, the overall resistance improvement is only attributed to the high  $n_s$  in the AlGaN barrier.

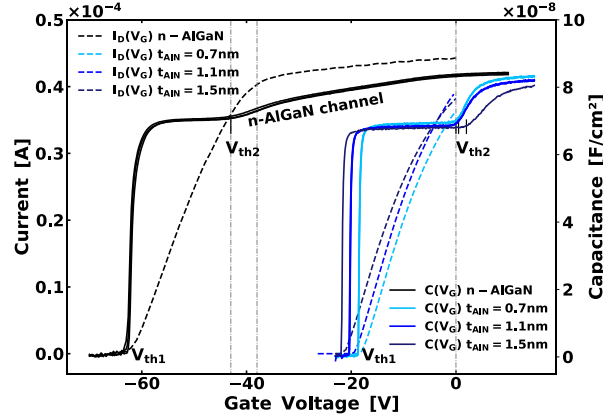


**Figure 2:**  $I_D(V_G)$  and  $C(V_G)$  measurements at 1kHz respectively on B1500 device analyzer and HP4284 LCR meter.

	$n_s$ ( $cm^{-2}$ )	$R_{2DEG}$ ( $\Omega/\square$ )	$\mu_s$ ( $cm^2 \cdot V^{-1} \cdot s^{-1}$ )
<b>A</b>	$7.9 \times 10^{12}$	371	2123
<b>B</b>	$8.2 \times 10^{12}$	344	2145
<b>C</b>	$8.4 \times 10^{12}$	351	1981
<b>D</b>	$8.2 \times 10^{12}$	441	1728

(a)

<b>D</b>	$n_s$ ( $cm^{-2}$ )	$R$ ( $\Omega/\square$ )	$\mu$ ( $cm^2 \cdot V^{-1} \cdot s^{-1}$ )
AlGaN channel	$2.1 \times 10^{13}$	1207	216
2DEG ( $V_G \sim -43V$ )	$8.2 \times 10^{12}$	441	1728
Total ( $V_G = 0V$ )	$2.9 \times 10^{13}$	323	663

(b)

**Table 1:** (a) Extracted 2DEG parameters  $R_{2DEG}$ ,  $n_s$  and  $\mu_s$  at  $V_G = 0V$  for samples A, B, C and at  $V_{th2}$  for sample D, (b) AlGaN and 2DEG detailed channel parameters for sample D.

	$t_{SiN}$ (nm)	$\sigma_{AlGaN/AlN}$ ( $cm^{-2}$ )	$\sigma_{AlN/GaN}$ ( $cm^{-2}$ )
<b>A</b>	73.5	$-6.00 \times 10^{12}$	$1.57 \times 10^{13}$
<b>B</b>	74.5	$-8.00 \times 10^{12}$	$1.82 \times 10^{13}$
<b>C</b>	75.5	$-1.42 \times 10^{13}$	$2.5 \times 10^{13}$
<b>D</b>	73.5	$-6.00 \times 10^{12}$	$1.57 \times 10^{13}$

**Table 2:** 1DSP simulated parameters for all samples. The fitting parameters are the interface charges  $\sigma_{AlGaN/AlN}$  and  $\sigma_{AlN/GaN}$  and the fitting references are  $V_{th1}$  and  $V_{th2}$ .

#### 4. Simulations

To understand the physical root causes leading to the enhancement of the 2DEG properties, the previous  $C(V_G)$  measurements are compared to 1DSP simulations and reported in **Figure 3**. The Poisson and Schrödinger equations are solved self-consistently under the parabolic mass approximation for the  $\Gamma$ -valley. The material parameters used in the simulations are based on Ref.7. The AlGaN polarization charge at the SiN/AlGaN interface is assumed to be completely compensated by a positive charge [7]. Polarization charges at the AlGaN/AlN and AlN/GaN interfaces ( $\sigma_{AlGaN/AlN}$  and  $\sigma_{AlN/GaN}$ ) are determined to account for the

experimental  $V_{th1}$  and  $V_{th2}$  and reported in **Table 2**. These charges are found to be lower than the theoretical values induced by AlN with complete polarization [8]. Indeed, theoretical charges are calculated according to the Ambacher's works [1,3,8], by considering two heterojunctions: the AlN/GaN heterojunction resulting in a positive polarization interface charge responsible for the well-known 2DEG, and the AlGaN/AlN heterojunction resulting in a negative polarization interface charge. The interface charges calculations take into account for the spontaneous ( $P_{sp}$ ) and the piezoelectric polarization ( $P_{pz}$ ). GaN is considered as a fully relaxed material. The theoretical charges values are very high ( $\sigma_{AlGaN/AlN} = -5.42 \times 10^{13} \text{ cm}^{-2}$  and  $\sigma_{AlN/GaN} = 6.56 \times 10^{13} \text{ cm}^{-2}$ ) and they induce a much more large shift on both  $V_{th1}$  (towards more negative voltage values) and  $V_{th2}$  (towards more positive voltage values) compared to the experimental results. In addition, not enough  $V_{th1}$  dependency with the AlN thickness is observed by considering these theoretical charges. Thereby, these results suggest that the polarization of AlN is attenuated for very thin layers. **Figure 4** illustrates the decrease of  $n_s$  with thinner AlN spacer. To take into account this reduction, we introduce a factor PR (polarization rate) in our calculations of polarization charges see Eq.6 and Eq.7. Interestingly, as depicted in **Figure 5**, using the same PR for the top and bottom charges, these calculated charges are similar to the ones extracted in **Table 2**, for the different  $t_{AlN}$ .

$$\sigma_{Al_xGa_{1-x}N/AlN}(x) = \{P_{tot}(AlN) \times PR - [P_{sp}(Al_xGa_{1-x}N) + P_{pz}(Al_xGa_{1-x}N)]\}/q \quad (6)$$

$$\sigma_{AlN/GaN} = \{P_{sp}(GaN) - P_{tot}(AlN) \times PR\}/q \quad (7)$$

These results support our assumption regarding the attenuation of the AlN polarization for very thin layer. Indeed, the theoretical charges calculation was demonstrated for thickness from 30nm [8]; in this work the studied thicknesses are approximately a few atomic layers considering that the lattice parameter  $c$  of the AlN is around 4.98Å. Another hypothesis is that this effect can also, in part, be due to a reduction of the Al fraction in AlN, which becomes an Al-rich AlGaN for very thin layers. However, this assumption seems not sufficient to explain the experimental observations. Indeed, both charges are interdependent and by decreasing the Al content and assuming a complete polarization, the simulated capacitance well reproduces the effect on the  $V_{th2}$  but not on  $V_{th1}$ . In addition, the Al molar fraction to account for the AlN/GaN polarization interface charge (**Tab.2**) are found to be too low, about 0.305, 0.35 and 0.46 respectively for the AlN 0.7nm, 1.1nm and 1.5nm and do not reproduce the  $V_{th1}$  variations.

Going back at **Table 2**, we can notice that for samples D and A, which differ only by AlGaN doping, the same interface charges are determined despite the very different  $V_{th1}$  and  $V_{th2}$  values obtained on the two samples. This is consistent and corroborates our estimations of  $\sigma_{AlGaN/AlN}$  and  $\sigma_{AlN/GaN}$ . **Figure 6** outlines the polarization rate reduction with thinner  $t_{AlN}$  through an empirical model. This simple model gives good approximation for simulations and it seems in accordance with Berdalovic's work, which supposes a 65% of polarization in a 3.5nm AlN layer.

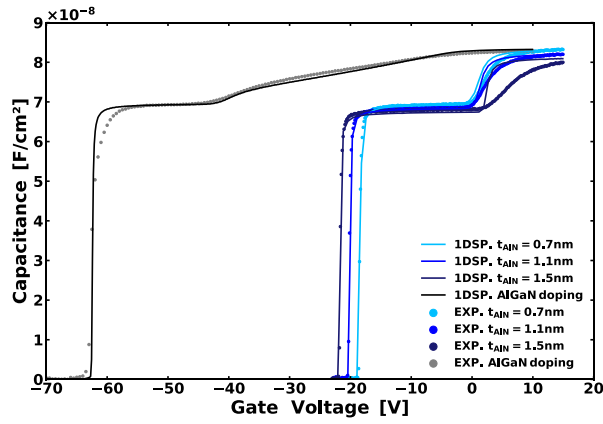


**Figure 3:**  $C(V_G)$  simulations (lines) and comparison with the experimental  $C(V_G)$  (dots) for samples A, B, C and D.

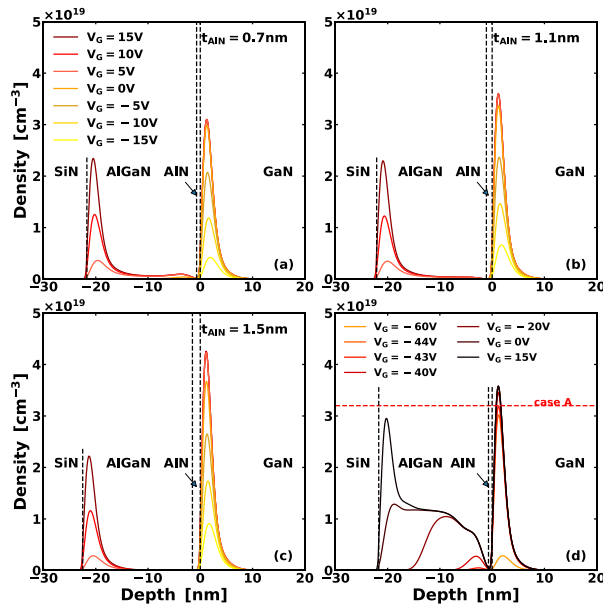


**Figure 4:** Electron density versus Depth at various  $V_G$  obtained from 1DSP simulations, (a) for  $t_{\text{AlN}}=0.7\text{nm}$ , (b) for  $t_{\text{AlN}}=1.1\text{nm}$ , (c) for  $t_{\text{AlN}}=1.5\text{nm}$ , (d) for the n-doped AlGaIn,  $t_{\text{AlN}}=0.7\text{nm}$ .

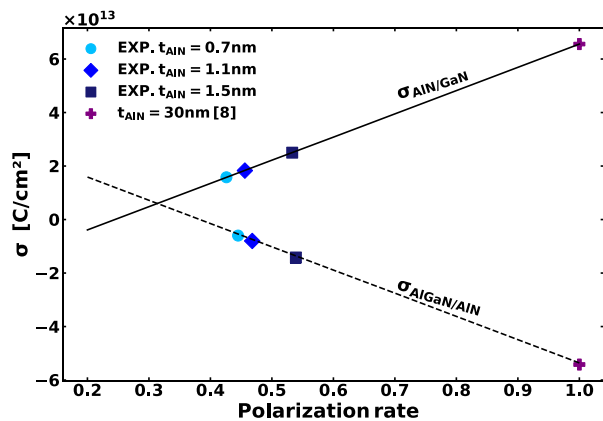


**Figure 5:** Lines:  $\sigma_{\text{AlGaIn/AlN}}$  and  $\sigma_{\text{AlN/GaN}}$  vs PR (Eq.6-7). Dots:  $\sigma_{\text{AlGaIn/AlN}}$  and  $\sigma_{\text{AlN/GaN}}$  extracted from measurements.

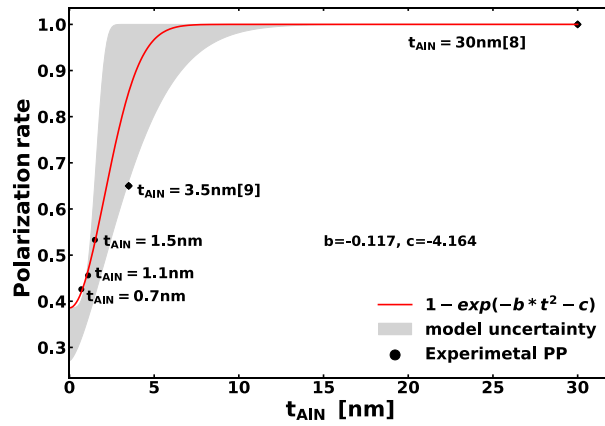


**Figure 6:** Empirical model predicting the evolution of the polarization rate in the AlN layer as a function of its thickness.

## 5. Conclusions

In summary, we have demonstrated that n-doped AlGa<sub>N</sub> improves the on state resistance due to the highly n-doped channel formation in AlGa<sub>N</sub> for negative voltages. We also showed that the 2DEG density was barely not affected by AlGa<sub>N</sub> n-doping. Then, we assumed that AlN polarization is attenuated for very thin layers, and increases with thicker AlN layers, resulting in a reduction of  $R_{2\text{DEG}}$ . This assumption seems the most suitable to explain experimental results. Nevertheless, we find out that  $R_{2\text{DEG}}$  enhancement with thicker AlN spacer is limited despite the ns improvement, by mobility degradation for  $t_{\text{AlN}}$  larger than 1.1nm.

## Acknowledgements

The authors would like to acknowledge the funding support from the PSPC French national program « G-Mobility ».

## REFERENCES

- [1] O. Ambacher et al., ‘Two-dimensional electron gases induced by spontaneous and piezoelectric polarization charges in N- and Ga-face AlGa<sub>N</sub>/Ga<sub>N</sub> heterostructures’, *Journal of Applied Physics*, vol. 85, pp. 3222–3233, 1999, doi: 10.1063/1.369664.
- [2] N. M. Shrestha, Y. Li, and E. Y. Chang, ‘Simulation study on electrical characteristic of AlGa<sub>N</sub>/Ga<sub>N</sub> high electron mobility transistors with AlN spacer layer’, *Japanese Journal of Applied Physics*, vol. 53, no. 4 SPEC. ISSUE, 2014, doi: 10.7567/JJAP.53.04EF08.
- [3] O. Ambacher et al., ‘Two dimensional electron gases induced by spontaneous and piezoelectric polarization in undoped and doped AlGa<sub>N</sub>/Ga<sub>N</sub> heterostructures’, *Journal of Applied Physics*, vol. 87, pp. 334–344, 2000, doi: 10.1063/1.371866.
- [4] F. Sonmez et al., ‘The effect of barrier layers on 2D electron effective mass in Al<sub>0.3</sub>Ga<sub>0.7</sub>N/AlN/GaN heterostructures’, *Journal of Physics: Condensed Matter*, vol. 33, p. 255501, 2021, doi: 10.1088/1361-648x/abf8d2.
- [5] A. Mondal, S. Ghosh, A. Roy, M. Kar, and A. Kundu, ‘Effect of Doped AlGa<sub>N</sub> Width Variation on Analog Performance of Dual Gate Underlap MOS-HEMT’, 2020, pp. 244–247. doi: 10.1109/CALCON49167.2020.9106535.

- [6] M. Wośko, B. Paszkiewicz, R. Paszkiewicz, and M. Tłaczała, ‘*Influence of growth process scheme on the properties of AlGaN/AlN/GaN heterostructures*’, *physica status solidi (c)*, vol. 10, pp. 306–310, 2013, doi: 10.1002/pssc.201200708.
- [7] B. Rustemi et al., ‘*Investigation on interface charges in SiN/Al<sub>x</sub>Ga<sub>1-x</sub>N/GaN heterostructures by analyzing the gate-to-channel capacitance and the drain current behaviors*’, *Journal of Applied Physics*, vol. 130, no. 10, 2021, doi: 10.1063/5.0058019.
- [8] O. Ambacher et al., ‘*Pyroelectric properties of Al(In)GaN/GaN hetero- and quantum well structures*’, *Journal of Physics: Condensed Matter*, vol. 14, pp. 3399–3434, 2002, doi: 10.1088/0953-8984/14/13/302.
- [9] I. Berdalovic, M. Poljak, and T. Suligoj, ‘*A comprehensive model and numerical analysis of electron mobility in GaN-based high electron mobility transistors*’, *Journal of Applied Physics*, vol. 129, no. 6, p. 064303, Feb. 2021, doi: 10.1063/5.0037228.